Molecular Biology of the Cell
Vol. 17, 1593–1605, April 2006

Cholesterol Is Required for Efficient Endoplasmic Reticulum-to-Golgi Transport of Secretory Membrane Proteins[V]

Andrew Ridsdale,* Maxime Denis,* Pierre-Yves Gougeon,* Johnny K. Ngsee,* John F. Presley,† and Xiaohui Zha*

*Ottawa Health Research Institute and University of Ottawa, Ottawa, Ontario K1Y 4E9, Canada; and †Department of Anatomy and Cell Biology, McGill University, Montreal, Quebec H3A 2B2, Canada

Submitted February 7, 2005; Revised January 19, 2006; Accepted January 20, 2006
Monitoring Editor: Sean Munro

Although cholesterol is synthesized in the endoplasmic reticulum (ER), compared with other cellular membranes, ER membrane has low cholesterol (3–6%). Most of the molecular machinery that regulates cellular cholesterol homeostasis also resides in the ER. Little is known about how cholesterol itself affects the ER membrane. Here, we demonstrate that acute cholesterol depletion in ER membranes impairs ER-to-Golgi transport of secretory membrane proteins. Cholesterol depletion is achieved by a brief inhibition of cholesterol synthesis with statins in cells grown in cholesterol-depleted medium. We provide evidence that secretory membrane proteins vesicular stomatitis virus glycoprotein and scavenger receptor A failed to be efficiently transported from the ER upon cholesterol depletion. Fluorescence photobleaching recovery experiments indicated that cholesterol depletion by statins leads to a severe loss of lateral mobility on the ER membrane of these transmembrane proteins, but not loss of mobility of proteins in the ER lumen. This impaired lateral mobility is correlated with impaired ER-to-Golgi transport. These results provide evidence for the first time that cholesterol is required in the ER membrane to maintain mobility of membrane proteins and thus protein secretion.

INTRODUCTION

Cholesterol is important in determining the physical properties of mammalian cellular membranes. By filling in the spaces between phospholipids in the bilayer of the membrane, cholesterol greatly influences properties such as membrane thickness, rigidity, and lateral organization (Silvius, 2003). The highest concentration of cholesterol in mammalian cells is found in the plasma membrane where it makes up 30–50% of total lipids and is important for mechanical rigidity (Lange, 1991). The endoplasmic reticulum (ER) membrane is cholesterol poor (3–6% of total lipids) (Lange, 1991). Interestingly, cholesterol is synthesized in the ER and is rapidly transported from the ER to other cellular membranes (Lusa *et al*., 2003). Importantly, most of the molecular machinery that regulates cellular cholesterol homeostasis resides in the ER membrane (Brown and Goldstein, 1999) and can apparently sense cholesterol (Brown and Goldstein, 1997). For example, the ER-resident protein sterol regulatory element–binding protein (SREBP) cleavage activation protein (SCAP) changes its conformation when there is a cholesterol deficiency in the ER membrane (Adams *et al*., 2003). This conformational change seems to be the direct physical cause whereby SCAP escorts SREBP to the Golgi for final processing.

What is directly sensed by SCAP remains obscure, although recent evidence suggests that SCAP senses cholesterol with its transmembrane domains. This implies that SCAP can detect cholesterol concentration in the ER membrane directly (Radhakrishnan *et al*., 2004), or, alternatively, that it can sense ER membrane properties (Adams *et al*., 2003). Relatively little is known, compared with the plasma membrane, about the properties of low-cholesterol membranes.

Depletion of cholesterol from the plasma membrane is known to have a significant effect on many cellular functions, including endocytosis, protein sorting, and signal transduction (Ikonen, 2001). Studies from model membranes with lipid compositions similar to the plasma membrane identified cholesterol as a critical factor influencing many membrane physical properties, including lateral organization (Silvius, 2003). These observations have inspired the popular concept of "microdomains" or "rafts" for the lateral organization of biological membranes rich in cholesterol (Simons and Toomre, 2000).

Relatively little is known about cholesterol's influence on the ER membrane. A limited number of studies on model membranes have indicated that the effects of cholesterol on cholesterol-poor membranes can be very different from those rich in cholesterol. For example, increased cholesterol is known to suppress Na^+ permeability of membranes containing high cholesterol (40%), but to enhance it in cholesterol-poor membranes (5%) (Corvera *et al*., 1992). Moreover, recent evidence from model membranes demonstrates that various physical properties of cholesterol-poor membranes

This article was published online ahead of print in *MBC in Press* (http://www.molbiolcell.org/cgi/doi/10.1091/mbc.E05–02–0100) on February 1, 2006.

[V] The online version of this article contains supplemental material at *MBC Online* (http://www.molbiolcell.org).

Address correspondence to: Xiaohui Zha (xzha@ohri.ca).

Abbreviations used: SREBP, sterol regulatory element–binding protein.

are highly sensitive to small cholesterol variations (Lemmich *et al*., 1997).

Even less is known about how cholesterol influences cholesterol-poor membranes in live cells, such as that of the ER. It is not clear whether membrane proteins made in the ER respond to cholesterol alteration in this environment. Variations in cholesterol content in the ER could influence the physical properties of the membrane, which could in turn impact on properties of membrane proteins, such as conformation and oligomerization. ER cholesterol alteration in vivo may also influence the transport of these membrane proteins into the vesicular secretory pathway.

Here, we describe the effects of acute cholesterol depletion, targeted to mainly influence the ER membrane, on vesicular transport of membrane proteins from the ER. We demonstrate that this depletion impairs vesicular stomatitis virus glycoprotein (VSVG) transport from the ER to the Golgi, and, concurrently, diminishes the lateral mobility of VSVG on the ER membrane. We also provide evidence that cholesterol depletion similarly influences lateral mobility of another secretory membrane protein, scavenger receptor A (SRA), on the ER membrane and its transport from the ER. We thus conclude that cholesterol is required for maintaining lateral mobility of secretory membrane proteins in the ER. Without such mobility these proteins could not effectively reach ER exit sites and thus fail to transport to the Golgi.

MATERIALS AND METHODS

Cell Culture and Reagents

Chinese hamster ovary (CHO) cells were grown in F-12 plus 5% fetal calf serum (FCS). CHO cells stably overexpressing green fluorescent protein (GFP)-ϵCOP were also grown in F-12 plus 5% FCS. Lipoprotein-deficient serum (LPDS) was prepared from FCS by density centrifugations (Pitas *et al*., 1981). Statins, mevalonate, 25-hydroxycholesterol, cholesterol, filipin, and cycloheximide were purchased from Sigma-Aldrich (St. Louis, MO). Anti-COPII and anti-β-COP were from Affinity Bioreagents (Golden, CO). Anti-ER-Golgi intermediate compartment (ERGIC)-53 was purchased from Alexis Biochemicals (Lausen, Switzerland). Anti-mannosidase II was originally from Dr. M. Farquhar (University of California, San Diego, San Diego, CA). Conformation-sensitive antibody against VSVG (I14) was kindly provided by Dr. M. Lyles (Wake Forest University, Winston-Salem, NC). Adenovirus encoding yellow fluorescent protein (YFP)-$VSVG_{ts045}$ was a gift from Drs. Keller and Simons (Max-Planck-Institute of Molecular Cell Biology and Genetics, Dresden, Germany). YFP-ER and YFP-Golgi DNA constructs were from (Clontech, Mountain View, CA). YFP-p58 was characterized previously (Presley *et al*., 2002). YFP-scavenger receptor type A construct was from Dr. Whitman (University of Ottawa Heart Institute, Ottawa, Ontario, Canada). Lipofectamine 2000 (Invitrogen, Carlsbad, CA) was used for all nonadenovirus transfections.

YFP-VSVG Transport Assay

CHO cells or fibroblasts were transfected with YFP-$VSVG_{ts045}$ and incubated at 39.5°C for 16–20 h to accumulate $VSVG_{ts045}$ in the ER. Statins were then added to the media and incubated for an additional hour. Cells were then transferred to 32°C for 10–20 min to allow VSVG to move to the Golgi and were fixed at the end of the 32°C incubation with 4% paraformaldehyde and analyzed by fluorescent microscopy.

YFP-SRA Transport Assay

CHO cells were transfected with YFP-SRA and incubated at 37°C for 10 h in either FCS or 5% LPDS-supplemented F-12 media. Statins were added to one-half of the wells for 30 min, and the remaining half served as control. This was followed by 2-h incubation in the presence of cycloheximide (from a 10 mg/ml ethanol stock, final concentration 10 μg/ml). Cells were then fixed with 4% paraformaldehyde, and images were taken with a 10× objective on a Nikon TE300 wide-field fluorescent microscope or with 60× (numerical aperture [NA] 1.4) objective on a Bio-Rad MRC 1024 confocal laser scanning microscope.

Acetyl-Low-Density Lipoprotein (LDL) Surface Binding Assay

Acetyl-LDL was first fluorescently labeled with Cy3 according to the manufacturer's instructions. CHO cells were transfected with YFP-SRA and incubated at 37°C for 10 h in 5% LPDS-supplemented F-12 media. Statins (40 μM) were added to one-half of the wells for 30 min, and the remaining half served as control. Cells were either cooled down on ice right away (t = 0 h) or incubated 2 h at 37°C in the presence of cycloheximide (10 μg/ml) before 30 min incubation on ice (t = 2 h). Ice-cold Cy3-acetyl-LDL (10 μg/ml) was added, and cells were further incubated on ice for 30 min to allow cell surface binding. Cells were then rinsed with ice-cold phosphate-buffered saline (PBS) three times to remove unbound Cy3-acetyl-LDL. For single cell analysis, cells were fixed with 4% paraformaldehyde and imaged by fluorescence microscopy using a charge-coupled device (CCD) camera to measure relative fluorescence intensity of YFP-SRA and Cy3-acetyl-LDL in individual cells. For biochemical analysis, cells were lysed with 1% Triton X-100 (TX-100)/SDS. Cy3 in the lysates was measured by fluorospectrometry. Lysates were also analyzed for their protein content to produce Cy3 fluorescence per milligram of cell protein.

Fluorescent Microscopy, Fluorescence Recovery after Photobleaching (FRAP), and Imaging Analysis

To measure the transport of YFP-VSVG, fluorescent images of fixed cells were acquired with either a Nikon TE300 fluorescence microscope using a 40× (NA 0.75) objective and cooled CCD camera (ORCA; Hamamatsu, Bridgewater, NJ) or Bio-Rad MRC 1024 confocal microscope. For live cell imaging, series of fluorescent images were acquired at 32°C with a Nikon TE 2000E inverted fluorescence microscope using a 60× objective (NA 1.4) and a cooled CCD camera (Cascade 512B EM; Photometrics, Tucson, AZ) operated by MetaMorph software (Universal Imaging, Downingtown, PA). For FRAP experiments, cells were grown in 40-mm glass-bottom dishes (Bioptechs, Butler, PA). After transfection and overnight incubation, these cells were transferred to a Bio-Rad MRC 1024 confocal microscope equipped with a Bioptechs FCS2 environmental chamber maintained at 39.5°C. The 488-nm line of an argon ion laser with a 60× (1.4 NA) objective was used. A defined square region was photobleached at full laser power (100%), and the recovery of fluorescence was monitored by scanning whole cells at low laser power (3–10%). Selected spots (2 × 2 μm) in the ER were photobleached by scanning for 3–5 s. The fluorescence recovery was then recorded as a time series (5 s per frame). Each experiment included a minimum of two independent trials performed over several months with each involving 10–20 individual repetitions of FRAP. Recovery of the fluorescent signal within the bleached spots was quantified using ImageJ software. A reference area outside of the photobleached area but in the same field of view was used to correct possible photobleaching during the time series recording.

Diffusion coefficients were determined by photobleach as described previously (Sciaky *et al*., 1997;Siggia *et al*., 2000). Briefly, a 3- × 3-μm square region was chosen in a flat area of a living cell away from the nucleus. A prebleach image was obtained of the entire cell before photobleach, and the square region was bleached with high-intensity laser light. A postbleach image was immediately obtained with subsequent images in a time series obtained at 5-s intervals. Diffusion coefficients were determined by comparing the actual recovery curve to a simulated recovery curve and appropriately scaling the temporal axis. This scaling was done automatically using a least-squares best fit. The algorithms and procedures used to create the simulated recovery curve and for the curve fit are described in detail (Siggia *et al*., 2000). The entire procedure was automated using computer software provided by E. Siggia (Rockefeller University, New York, NY; Siggia *et al*., 2000). An important advantage of this method is that it does not require detailed knowledge of the geometry of the bleach and can be used even when the bleach area is large compared with the size of the cell. Both simulated and actual recovery curves were expressed in terms of fraction of total cellular fluorescence in the bleach area as a function of time.

VSV-G_{ts045} Endoglycosidase H (Endo H) Trafficking Assay

CHO cells were transfected with a pcDNA3.1+/VSV-G_{ts045} construct using Lipofectamine. Cells were grown overnight in F-12 with 5% fetal calf serum or LPDS. Cells were shifted to 42°C for 6 h. At the 5-h time point, 40 μM statin was added to one-half the wells, and 15 min before the temperature shift, 20 μM cycloheximide was added to all the wells. Cells were then shifted to 32°C for 0 or 30 min. At each time point, the cells were washed in PBS, scraped in PBS with a rubber policeman and collected by a 5-min 1500 rpm spin. The cells were then resuspended in 200 μl of 20 mM Tris-HCl, pH 7.5, and lysed by sonication. Cell debris was removed by a 5-min 2500 rpm spin. The VSVG containing membranes were collected by high-speed centrifugation (48,000 rpm; TLA 120.2) of the supernatant. The resulting pellets were resuspended by sonication in 200 μl of 50 mM trisodium citrate, 0.2% SDS. The samples were then boiled and treated overnight with 5 mU endo H (Roche Diagnostics, Indianapolis, IN), except for the two controls without endo H. The samples were trichloroacetic acid precipitated, resuspended in SDS sample buffer, run on 7.5% polyacrylamide gels, and transferred onto nitrocellulose membranes. The membranes were blocked with 5% skim milk powder in Tris-buffered saline (TBS)-Tween, incubated with rabbit anti-VSVG primary antibodies (Stressgen Biotechnologies, Victoria, British Columbia, Canada), washed with TBS-Tween, incubated with Alexa Fluor 488 goat anti-rabbit secondary antibodies (Molecular Probes, Eugene, OR), washed again, and the

VSVG protein was visualized using the Typhoon 8600 (Molecular Dynamics, Sunyvale, CA).

Detergent Solubility

To measure detergent solubility, YFP-VSVG$_{ts045}$–transfected CHO cells were cooled on ice immediately after being removed from the 39.5°C incubator. After 30 min on ice, cells were either fixed with 4% paraformaldehyde or further treated with 1% ice-cold TX-100 for 30 min. After rinsing with cold PBS three times, cells were immediately observed by fluorescent microscopy. Cells transfected with YFP-GPI and YFP-VSVG were used as controls. Under our experimental conditions, the plasma membrane YFP-GPI largely remained, indicating detergent insolubility. YFP-VSVG on the plasma membrane was completely removed.

RESULTS

Cholesterol Depletion in the ER by Inhibition of Cholesterol Synthesis Greatly Reduces VSVG ER-to-Golgi Transport

To specifically deplete cholesterol in the ER, we took advantage of the fact that cells grown in LPDS entirely depend on endogenous synthesis of cholesterol to sustain cell growth. Such condition in CHO cells is known to activate SCAP, thereby triggering endogenous cholesterol synthesis in the ER (Brown and Goldstein, 1999; Adams *et al*., 2003). Cholesterol was then transported to other cellular locations, including the Golgi and the plasma membrane (Heino *et al*., 2000). Because cholesterol made in the ER is the sole source of cholesterol in these cells, we reasoned that a brief inhibition of cholesterol synthesis in these cells should lead, initially, to acute cholesterol depletion of the ER pool. We therefore treated LPDS-grown CHO cells for 1 h with statins, specific inhibitors of 3-hydroxy-3-methylglutaryl (HMG)-CoA reductase, a key enzyme in the cholesterol biosynthesis pathway (Istvan, 2003). This treatment decreased cellular free cholesterol content by <30% (0.32 ± 0.049 versus 0.23 ± 0.013 μg/mg protein). Importantly, statin treatment under our experimental condition is a much gentler approach in comparison with commonly used methyl-β-cyclodextrin (MCD), which routinely depletes ~60% of cellular cholesterol (Keller and Simons, 1998). Another important distinction is that MCD is known to absorb cholesterol from the plasma membrane and any effect of MCD on intracellular organelles most likely is secondary to the initial events on the plasma membrane. Statin treatment, on another hand, should decrease cholesterol in the ER membrane initially, which, given enough time, may propagate to other cellular organelles. We therefore treated cells with statin for only 1 h, attempting to confine cholesterol depletion mainly to the ER. We chose 1-h statin treatment because it was shown previously that, in CHO cells, [^{3}H]acetate, an early precursor for synthesizing cholesterol, was significantly converted to [^{3}H]cholesterol in <1 h (Bradfute and Simoni, 1994). We reasoned that 1-h inhibition of HMG-CoA reductase should diminish cholesterol output significantly and yet minimize the disturbance. Indeed, we detected a decrease of cholesterol in statin-treated cells as described above and, when we stained cholesterol in these cells with filipin, we did not find dramatic alterations in cholesterol distribution (Figure 1 A, a and c). Filipin stain in CHO cells is well characterized to mark cholesterol-rich compartments such as the plasma membrane, recycling endosomes and the Golgi (Mukherjee *et al*., 1998). We found that these features were equally prominent in statin-treated cells compared with controls (see arrows for the Golgi and arrowheads for the recycling endosomes). These observations assured us that the cholesterol contents in the plasma membrane and in the Golgi were not greatly altered in statin-treated cells. As expected, MCD treatment significantly changed the appearance of filipin with diminished plasma membrane and decreased Golgi staining (Figure 1A, b). We thus concluded that, unlike MCD, acute statin treatment most likely depletes cholesterol primarily from the ER.

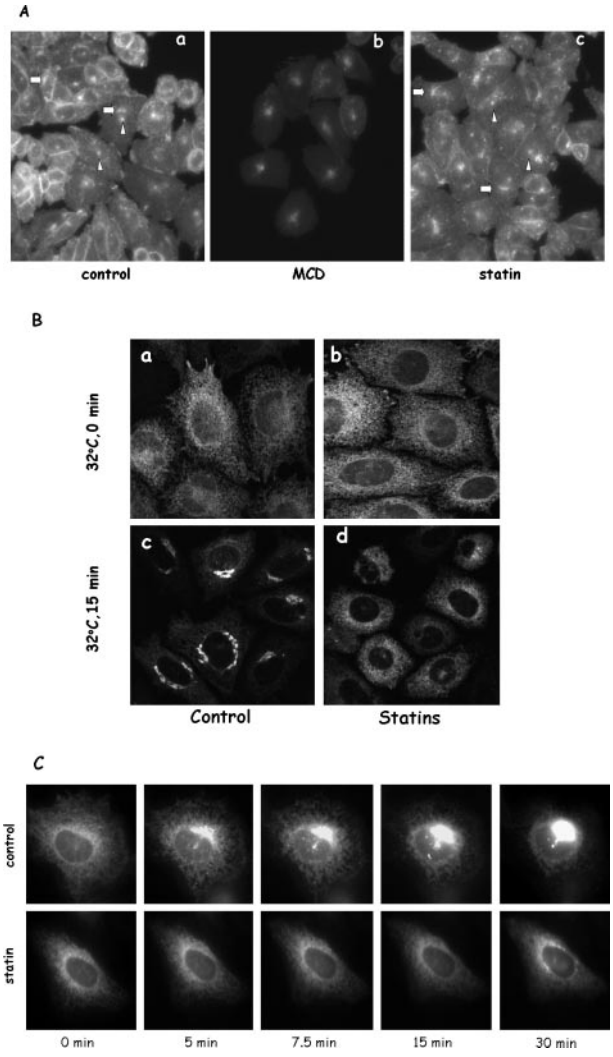

Figure 1. Cholesterol depletion by statin impairs VSVG transport from the ER to the Golgi in LPDS-grown CHO cells. (A) CHO cells grown in LPDS were treated with either 10 mM MCD for 30 min or 40 μM lovastatin for 1 h at 37°C. Cells were then fixed and stained with filipin. Images were taken and displayed under identical conditions. Arrows are for the Golgi, and arrowheads are for recycling endosomes. (B) CHO cells grown in LPDS were transfected with YFP-VSVG and incubated at 39.5°C overnight. Cells were then incubated with medium containing lovastatin (40 μM) for 1 h at 39.5°C before being moved to a 32°C incubator for 15 min. Cells were again fixed with 4% paraformaldehyde before microscopy observation. In addition to lovastatin, cells treated with 10 μM simvastatin or 70 μM compactin produced similar effects. (C) VSVG-transfected cells were treated with or without statin for 1 h at 39.5°C before being moved to a microscope stage controlled at 32°C.

We then asked whether the vesicular transport of a glycoprotein with a single transmembrane domain, VSVG, is affected by statin treatment. CHO cells grown in LPDS were transfected with YFP-VSVG$_{ts045}$ (Keller *et al*., 2001). This YFP-tagged variant of VSVG is retained in the ER at 39.5°C (t = 0; Figure 1B, a and b) because of a temperature-sensitive misfolding, but it can be folded normally and transported to the Golgi at 32°C (Bergmann, 1989; Keller *et al*., 2001). Figure

1B shows that, upon releasing the temperature block, the majority of VSVG moves from the ER to the Golgi within 15 min at 32°C (c). When we treated these LPDS-grown CHO cells with statin for 1 h before switching cells to 32°C, however, we found that VSVG transport from the ER to the Golgi in statin-treated cells was profoundly impaired. The majority of VSVG remained in the ER for the same 15 min (Figure 1B, d). A time course of VSVG movement in live cells with or without statin treatment is shown in Figure 1C. We observed that, upon temperature release, VSVG in control cells was rapidly concentrated in distinctive spots, presumably the ER exit sites, before moving to the Golgi (see Supplemental Movie 1). In statin-treated cells, however, VSVG retained its reticular appearance with no significant movement toward either ER exit sites or the Golgi (Supplemental Movie 2). Similar inhibition of VSVG transport by statin was also observed in human primary fibroblasts (our unpublished data). Moreover, we tested various statins (lovastatin, compactin, and simvastatin) and found identical inhibition by all, indicating a direct effect of cholesterol synthesis inhibition.

Statins Do Not Significantly Alter Vesicular Transport in FCS-grown Cells

Cells grown in FCS do not depend on endogenous cholesterol synthesis for their growth and express much less of the enzymes involved in cholesterol synthesis, including HMG-CoA reductase, the direct target of statins. Thus, VSVG transport in FCS-grown cells should not be as significantly affected by statins. Indeed, when FCS-grown cells were treated with statins, VSVG was transported normally to the Golgi by the end of the 15-min incubation at 32°C (Figure 2A, b).

To quantitatively evaluate VSVG transport, we assessed the process by VSVG endo H sensitivity. Secretory proteins, such as VSVG, should acquire endo H resistance once they have reached the Golgi. As shown in Figure 2B, >60% of VSVG became endo H resistant in control cells (both FCS and LPDS grown) after 30 min at 32°C, indicating that the majority of VSVG had reached the Golgi. In LPDS-grown cells treated with statin, however, only ~20% of the VSVG gained resistance (Figure 2B, b). Statin only exerted a slight influence on VSVG transport in FCS-grown cells, consistent with our above-described morphological observations (Figure 2A).

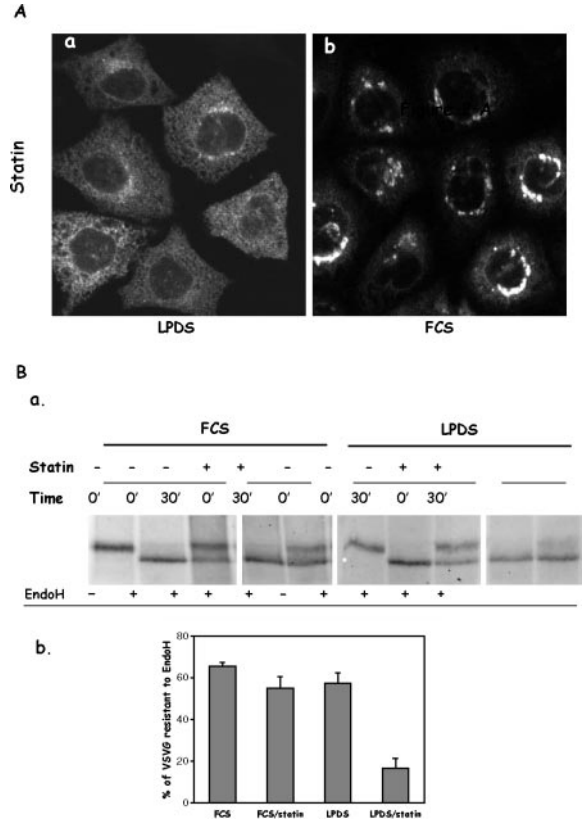

Figure 2. Cholesterol depletion by statin had little effect on VSVG transport from the ER to the Golgi in FCS-grown CHO cells. (A) CHO cells grown in LPDS (a) or FCS (b) were transfected with YFP-VSVG and incubated at 39.5°C overnight. Cells were treated with 40 μM lovastatin for 1 h before a 15-min incubation at 32°C. (B) Cells transfected with VSVG were treated with or without 40 μM statin for 1 h before shifting to 32°C for 30 min. Cells were lysed and divided to two equal portions. One portion was treated with 5 mU endo H. After precipitation, Western blot was performed, and VSVG was probed by anti-VSVG primary antibody (a). Bands were quantified, and endo H resistance was presented as percentage of endo H-resistant VSVG over total VSVG (b).

Cholesterol Biosynthetic Intermediates Downstream of HMG-CoA Reductase Rescue the Transport

If impaired vesicular transport is because of the inhibition of HMG-CoA reductase by statins, exogenously added intermediates downstream of HMG-CoA reductase in cholesterol synthesis pathway should be able to rescue the impaired transport. When we supplemented LPDS media with mevalonate, the direct product of HMG-CoA reductase, during statin treatment, we indeed found that mevalonate was able to overcome the statin effect and rescue the transport. VSVG was transported to the Golgi normally (Figure 3A, b).

Mevalonate is also a precursor of isoprenoid intermediates (Goldstein and Brown, 1990), which are required for posttranslational modifications of many proteins, including small G proteins, such as these in the Ras and Rho families (Van Aelst and D'Souza-Schorey, 1997). These proteins are known to be involved in vesicular transport (Hall, 1998). We therefore tested whether statin-induced transport inhibition is because of the depletion of isoprenylated proteins. For this purpose, we inhibited protein synthesis for 1 h, the same time interval as the statin treatment, to determine whether the existing pool of isoprenylated proteins is sufficient to support vesicular transport. As shown Figure 3A, d, 1-h treatment with a general protein synthesis inhibitor, cycloheximide, had little effect on ER VSVG vesicular transport to the Golgi. This indicates that new protein synthesis is not required for ER-to-Golgi vesicular transport within our experimental time frame. Newly synthesized proteins, such as small G proteins, are posttranslationally modified immediately after synthesis and most of them exist in isoprenylated form in cells at steady state as prenylation is known to be irreversible (Hancock *et al*., 1989; Schafer and Rine, 1992). Cycloheximide treatment can thus be broadly interpreted as an inhibition of isoprenylated protein synthesis. Statin-induced inhibition of vesicular transport is therefore not likely because of lack of isoprenoid intermediates.

Most importantly, we found that cholesterol itself could rescue the transport. When a small amount of cholesterol from a 10 mg/ml ethanol stock was added to the medium (final concentration 1 μg/ml) with statin, VSVG transport was completely restored (Figure 3A, f). A similar restoration was also observed when we used 25-hydroxycholesterol/cholesterol (our unpublished data), the combination shown

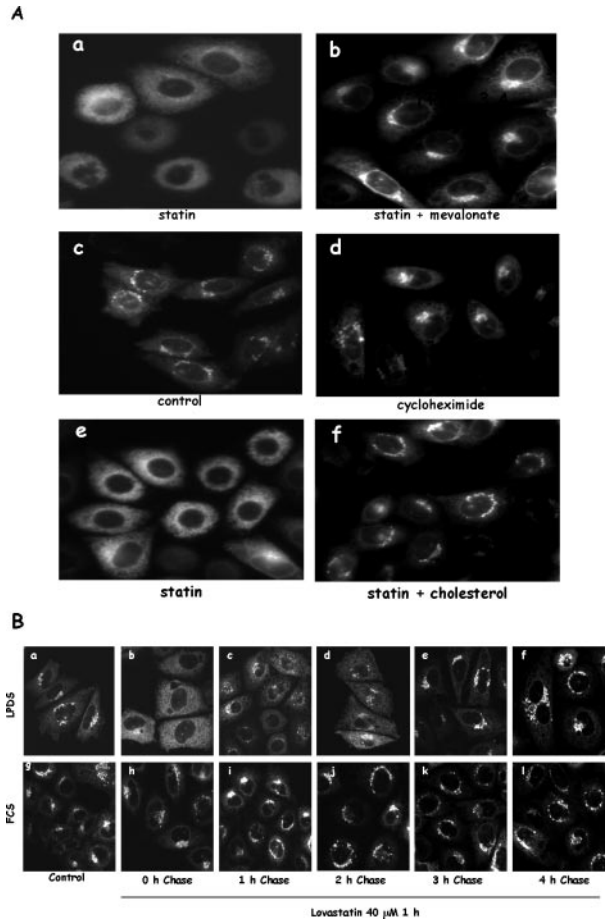

Figure 3. Impaired VSVG vesicular transport can be rescued by mevalonate and cholesterol. (A) CHO cells were grown in LPDS and transfected with YFP-VSVG. Cells were then treated with 40 μM lovastatin for 1 h with (b) or without 25 μM mevalonate (a) before a 15-min incubation at 32°C. Some of the cells were treated with 20 μg/ml cycloheximide only (d) or statin plus cholesterol (1 μg/ml) for 1 h (f) before the 15-min incubation at 32°C. (B) CHO cells grown in LPDS or FCS were transfected with YFP-VSVG and treated with 40 μM lovastatin for 1 h at 39.5°C. Cells were then either immediately transferred to 32°C for 15-min incubation (b and h) or changed to normal growing media without statin for the indicated time (c–f and i–l) at 39.5°C before 15-min incubation at 32°C. Cells were fixed before microscopic observation. Cells without statin treatment (control) are shown in a and g.

by others to efficiently supply cholesterol to the ER and inactivate SREBPs in CHO cells (Adams *et al*., 2003).

Furthermore, we found that cells treated with statin were perfectly viable. We treated cells with statin for 1 h and then changed them into statin-free media for the indicated times. VSVG transport form the ER to the Golgi was rapidly resumed upon removing statin. By 3 h, these cells were indistinguishable from control cells (Figure 3B).

Golgi Structure/Function and ER Exit Sites Are Not Significantly Altered by Statin Treatment in LPDS-grown Cells

There are several possible mechanisms that may impair VSVG transport. For example, the Golgi apparatus might have been disassembled by statin treatment. To address this issue, we first expressed a Golgi marker protein, YFP-Golgi, that contains the N-terminal 81 amino acids of human β1,4-galactosyltransferase, in both FCS- and LPDS-grown cells. As shown in Figure 4A, the Golgi structure in LPDS-grown cells treated with statin was slightly fragmented (Figure 4A, d) in comparison with control cells (Figure 4A, c). The majority of the Golgi structure, however, seemed to be intact and, importantly, was no more fragmented than in FCS-grown cells treated identically with statin (Figure 4A, b). These FCS-grown cells had nearly normal VSVG ER-to-Golgi transport, suggesting that this low degree of Golgi fragmentation is not directly related to vesicular transport. In addition, VSVG can eventually reach the Golgi in LPDS-grown cells treated with statin, albeit at a much slower rate (our unpublished data).

We also performed a series of immunostaining for endogenous proteins that are either resident proteins of the secretory pathway or coating component for vesicular transport between the ER and the Golgi. In statin-treated LPDS-grown CHO cells, we found that the localization of mannosidase II, a Golgi-resident enzyme, seemed not to be significantly different from that of control cells (Figure 4B, first row). The cellular distribution of β-COP, a cytosolic coating protein that reversibly binds to budding vesicles predominantly in the Golgi, also seemed largely normal in statin-treated cells (Figure 4B, second row). To ensure that cholesterol depletion by statin did not exert significant effect on ER exit sites, we stained for COPII. Secretory proteins exit ER mainly by budding vesicles coated by COPII (Antonny and Schekman, 2001). Cholesterol depletion by statin may disassemble ER exit sites and disperse COPII, thus dismantling vesicular transport. We found, however, that COPII was still concentrated on the punctate structures in the ER membrane in statin-treated cells with an appearance indistinguishable from controls (Figure 4B, third row). This suggests that the exit sites are still largely intact. Furthermore, we wondered whether ERGIC was intact in statin-treated cells. We first tried monoclonal antibody (mAb) G1/93 (Schweizer *et al*., 1988) and found this antibody not to recognize endogenous p58/ERGIC-53 in CHO cells. Signals were weak, and we did not observe any significant Golgi structures (our unpublished data). This may reflect tissue specificity of the antibody. We then expressed YFP-p58 (Presley *et al*., 2002) in CHO cells and examined its distribution upon statin treatment. In control cells, as shown in Figure 4C, YFP-p58 is primarily localized in the Golgi in addition to numerous cytosolic punctate spots, presumably the ERGIC (Figure 4C, a). ER was only faintly visible. In statin-treated cells, Golgi and ERGIC were still predominantly visible, but there was now much more YFP-p58 in the ER (Figure 4C, b). This shift of relative distribution was further quantified by taking fluorescence intensity ratio of YFP-p58 between Golgi and ER from a large number of single cells. Results shown in Figure 4C, c demonstrate that only one-half as much YFP-p58 in the Golgi relative to the ER (smaller Golgi/ER ratio) in statin-treated cells. This observation likely suggests two things. First, the Golgi itself is still structurally intact in statin-treated cells, consistent with our above-mentioned observations with other Golgi markers. Second, more YFP-P58 is in the ER may reflect a slower ER exit in statin-treated cells. P58/ERGIC53 is known to contain a strong sorting signal that facilitates its efficient exit from the ER while rapidly recycling between ER and Golgi (Kappeler *et al*., 1997). This may provide p58 an advantage such that, although also slowing down to some degree by statin, p58 can still exit the ER with a higher efficiency than other proteins, such as VSVG, to maintain its Golgi localization. This, together with our results using other Golgi markers, led us to

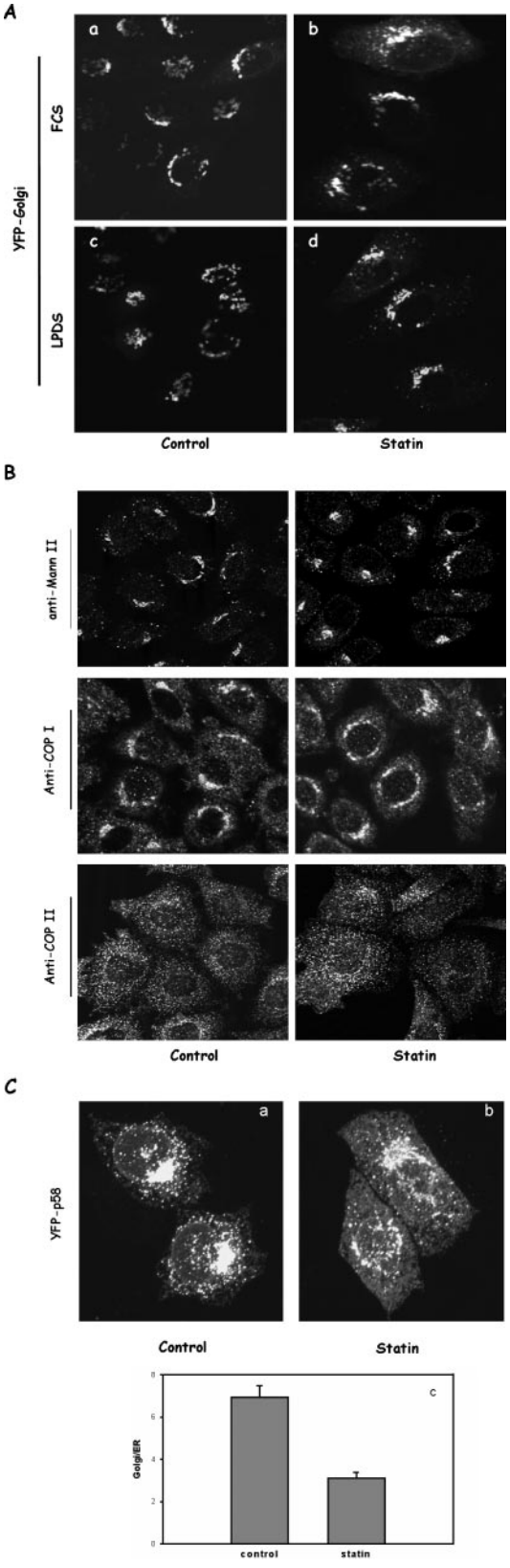

Figure 4. The Golgi and ER exit sites remain intact in statin-treated cells. (A) CHO cells grown in LPDS or FCS were transfected with YFP-Golgi. Some cells were treated with 40 μM lovastatin for 1 h (b and d) before confocal microscopy. (B) CHO cells grown in LPDS were treated with 40 μM lovastatin or without (control) for 1 h. Cells were then fixed and immunostained for mannosidase II (first row), β-COP (second row), and COP II (third row). Antibodies were detected with Alexa 488 secondary antibodies against either mouse or rabbit. (C) CHO cells transiently expressing YFP-p58 were treated with 40 μM lovastatin for 1 h or without (control) before paraformaldehyde fixation. Cells were then imaged by confocal microscopy as z-series through out the cells volume. The z-projection images are shown (a and b). For single cell analysis in c, cells were imaged by wide-field fluorescence microscopy. The average fluorescence intensities from the Golgi and ER were taken and presented as Golgi/ER ratio to measure relative distribution. Each data point represents the average from more than 60 single cells and error bars are SEM.

conclude that 1-h statin treatment did not significantly disrupt Golgi structure.

To further ensure that the Golgi is functionally active in statin-treated cells, we examined by live cell imaging Golgi coat protein movements in CHO cells stably expressing ϵCOP-GFP (Presley *et al*., 2002). ϵCOP-GFP was predominantly located in the Golgi in both control and statin-treated cells (Figure 5A), consistent with our earlier β-COP immunostaining. ϵCOP-GFP in control cells was seen actively moving to and from the Golgi in small punctate structures (Supplemental Movie 3). Similar movements were observed in cells treated with statin (Supplemental Movie 4). These observations imply that statin treatment did not significantly affect vesicular processes between the ER and the Golgi.

We next characterized, in LPDS-grown cells, VSVG vesicular transport from the Golgi to the plasma membrane, a process known to be sensitive to cholesterol. It was achieved by applying a 19.5°C temperature block to allow VSVG to accumulate in the Golgi (Figure 5B, a and c) and statin was added for the last hour (Figure 5B, c and d). This was followed by 15-min incubation at 32°C. A portion of VSVG could be seen to have reached the plasma membrane by the end of 15 min in both control and statin-treated cells (Figure 5B, b and d). We did not observe a significant influence of statin on Golgi-to-plasma membrane transport of VSVG.

To further dissect impaired VSVG transport from the ER, we asked whether VSVG could reach ERGIC. CHO cells expressing VSVG were treated with or without statin for 1 h at 40°C before shifting to 15°C for an additional 2 h. As expected, a large portion of VSVG in control cells was in the ERGIC (Figure 5C, a). VSVG in statin-treated cells, however, remained in the ER (Figure 5C, b), indicating an impaired transport to intermediate compartments. When we analyzed a large number of cells, we found that VSVG had a predominant ERGIC localization in 99% control cells, whereas ERGIC was visible only in ~10% statin-treated cells (Figure 5C, c). Because ERGIC was largely intact in these statin-treated cells (Figure 4C, b), impaired VSVG transport is most likely because of failure of ER exit.

Together, evidence presented above suggests that impaired VSVG transport from the ER is not because of disintegration of the Golgi. Cholesterol depletion by statin thus most likely directly influences the ER, particularly the ER membrane.

The ER Mobility of VSVG, but Not Lumen Proteins, Is Severely Reduced by Statin Treatment in LPDS-grown Cells as Demonstrated by FRAP

Because cholesterol depletion in the ER most likely alters membrane physical properties, we reasoned that statins may influence VSVG lateral mobility on the ER membrane. We therefore characterized VSVG mobility on the ER membrane using FRAP. As shown in Figure 6A, top row, VSVG fluo-

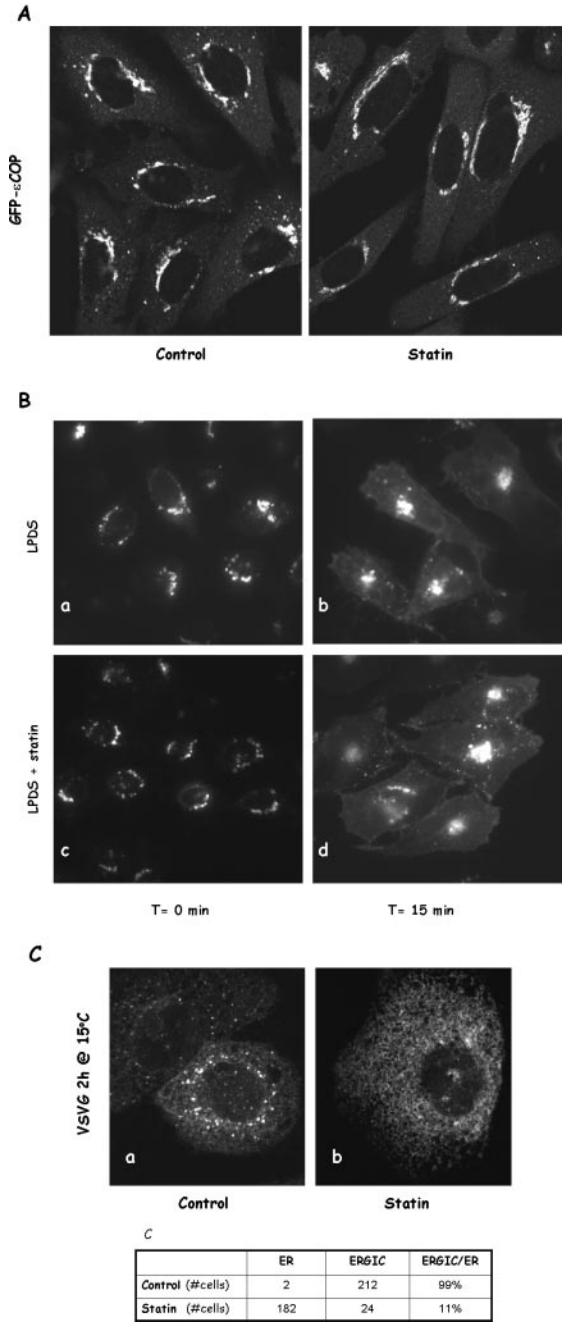

C

	ER	ERGIC	ERGIC/ER
Control (#cells)	2	212	99%
Statin (#cells)	182	24	11%

Figure 5. The Golgi is largely functional in statin-treated cells. (A) CHO cells stably expressing GFP-ϵCOP were treated with 40 μM lovastatin for 1 h or without (control) before confocal microscopy imaging. (B) LPDS-grown CHO cells were transfected with VSVG and incubated at 39.5°C overnight. Cells were then moved to a 19.5°C for 2 h to accumulate VSVG in the Golgi. Statin (40 μM) was added to half of the wells for the last hour. This was followed by 15 min at 32°C before fixing and microscopic observation. (C) LPDS-grown CHO cells were transfected with VSVG and incubated at 39.5°C overnight and statin was added for the hour (b). Cells were then moved to 15°C for 2 h to accumulate VSVG in the ER/Golgi intermediate compartment. Cells were also scored for the appearance of punctate dots (ERGIC) in the cytoplasm (c).

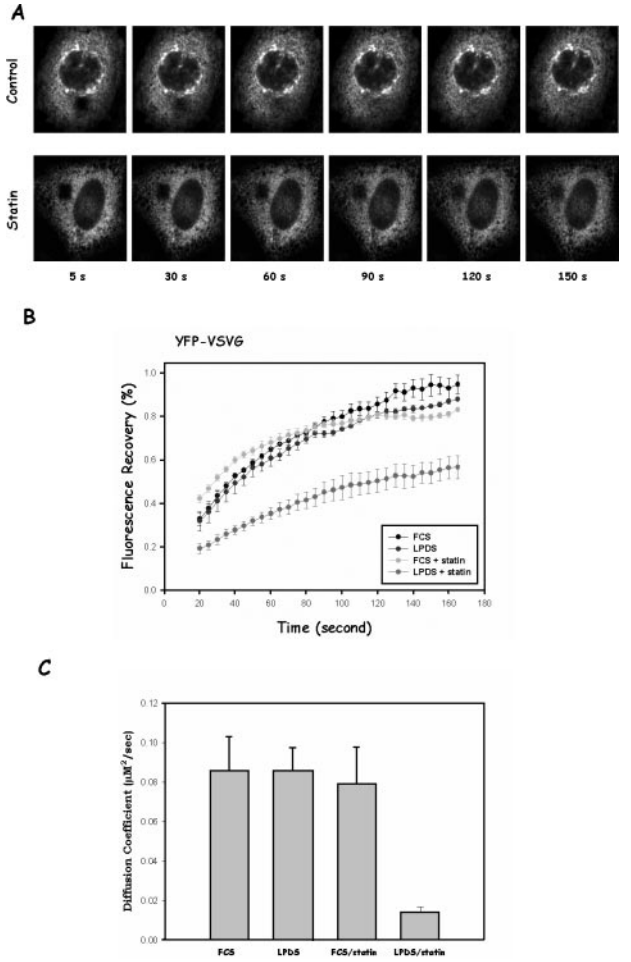

Figure 6. Cholesterol depletion by statin impairs lateral mobility of VSVG but not lumen protein. (A) CHO cells were transfected with YFP-VSVG and incubated at 39.5°C overnight. Cells were then either treated with lovastatin (bottom row) for 1 h or without (top row) before being transferred to microscope stage for FRAP measurements. Images were obtained at indicated time points after photobleaching. (B) Quantitative analysis of YFP-VSVG fluorescence recovery in the ER. The fluorescence intensities from photobleached spots were plotted as percentage of prebleach intensity in the same area against time. Each curve represents the average from five to 10 cells. Error bars are SEM. (C) Diffusion coefficient from each treatment.

rescence in photobleached area was quickly recovered in control LPDS-grown cells, consistent with previous observations (Nehls *et al*., 2000). In contrast, we found that the bleached area was recovered much more slowly, when cells were treated with statin. Even at 150 s, the bleached area was still clearly visible (Figure 6A, bottom row).

Quantification of the FRAP experiments is shown in Figure 6B. In cells grown in FCS or LPDS without statin, YFP-VSVG demonstrated similar recovery curves after bleaching. Fluorescence recovery of YFP-VSVG in statin-treated LPDS-grown cells after identical photobleaching was much slower. This is also reflected by their diffusion coefficients, shown in Figure 6C. The diffusion coefficient D for control cells is 0.085 ± 0.017 $\mu m^2/s$, which is largely consistent with other membrane proteins in the ER, including VSVG (Haggie *et al*., 2002). In statin-treated, LPDS-grown cells, however, D is 0.014 ± 0.002 $\mu m^2/s$, ~20% of controls. This strongly suggests that statin slows down the lateral diffusion of VSVG on the ER membrane. The decreased lateral mobility thus seems to be correlated with the deficiency of VSVG ER-to-Golgi

transport. In support of this correlation, VSVG in FCS-grown cells remained mobile even when treated with statins (Figure 6, B and C), indistinguishable from control cells. This is consistent with our earlier observation that VSVG transport was not significantly affected by statin in these cells (Figure 2B).

The loss of lateral mobility is not likely because of VSVG misfolding by statin at the permissive temperature (32°C). In fact, misfolded VSVG was known to remain perfectly mobile in the ER membrane, indistinguishable from correctly folded VSVG (Nehls *et al*., 2000). Nevertheless, misfolding could still contribute at least in part to impaired VSVG transport. We therefore examined whether cholesterol depletion by statin influences VSVG folding, which could impact on VSVG ER exit independently of lateral mobility. We found that a similar amount of VSVG was correctly folded after 15 min at 32°C, judging by staining with I14, a folding-sensitive VSVG antibody (Lefrancios and Lyles, 1982), in both control and statin-treated cells (Figure 7A, e–h). As expected, I14 did not recognize misfolded VSVG at 40°C (Figure 7A, a–d). We then quantified the relative fluorescence intensity of I14 (correctly folded VSVG) versus the fluorescence intensity of YFP (total VSVG) to estimate the folding efficiency and found that the folding efficiency in statin-treated cells was only slightly less than that in control cells (Figure 7B). To further ensure the folding kinetics is not altered by statin, we also performed a time course of VSVG folding in control or statin-treated cells (Figure 7B, inset). On switching to 32°C, VSVG rapidly resumed its correct conformation with $t_{1/2}$ of 1–2 min, in agreement with a previous study (de Silva *et al*., 1990). The folding efficiency in statin-treated cells was again ~85% of that in control cells in all the time points examined. This slight decline of VSVG folding could contribute to a slightly delay in VSVG transport from the ER. However, >80% of VSVG is correctly folded after statin treatment. VSVG misfolding at the permissive temperature, therefore, could not be the main cause for impaired VSVG ER-to-Golgi transport. Interestingly, correctly folded VSVG seemed to be more aggregated in appearance, which may reflect the relative immobility of these proteins on the ER membrane because of cholesterol depletion.

We also considered the possibility that cholesterol depletion in the ER by statins may break the ER reticulum network, which could also lead to the apparent loss of lateral mobility of membrane proteins. To address this, an ER lumen protein, YFP-ER (KDEL signal attached to YFP), was expressed in CHO cells. We found that the lateral mobility of YFP-ER was not affected by statin treatment in either LPDS or FCS-grown cells (Figure 7C). Additionally, we observed that the lateral mobility of another lumen protein, GFP-prolactase, was also not affected by statin treatment in the ER (our unpublished data). Evidence thus indicated that the loss of lateral mobility of membrane proteins by statin is due to changes in the ER membrane, not a general structural disintegration.

Another Secretory Membrane Protein, SRA, Also Loses Mobility in the ER after Statin Treatment, and, Concurrently, Fails to Be Efficiently Transported Out of the ER

To further verify that cholesterol depletion in the ER has a general effect on secretory membrane proteins, we characterized the effect of statin on another secretory membrane protein by measuring both lateral mobility and vesicular transport. YFP-scavenger receptor A (YFP-SRA) is a type I transmembrane protein that normally localizes on the plasma membrane and has no known defect in protein folding. As shown in Figure 8A, shortly after transfection (t = 0),

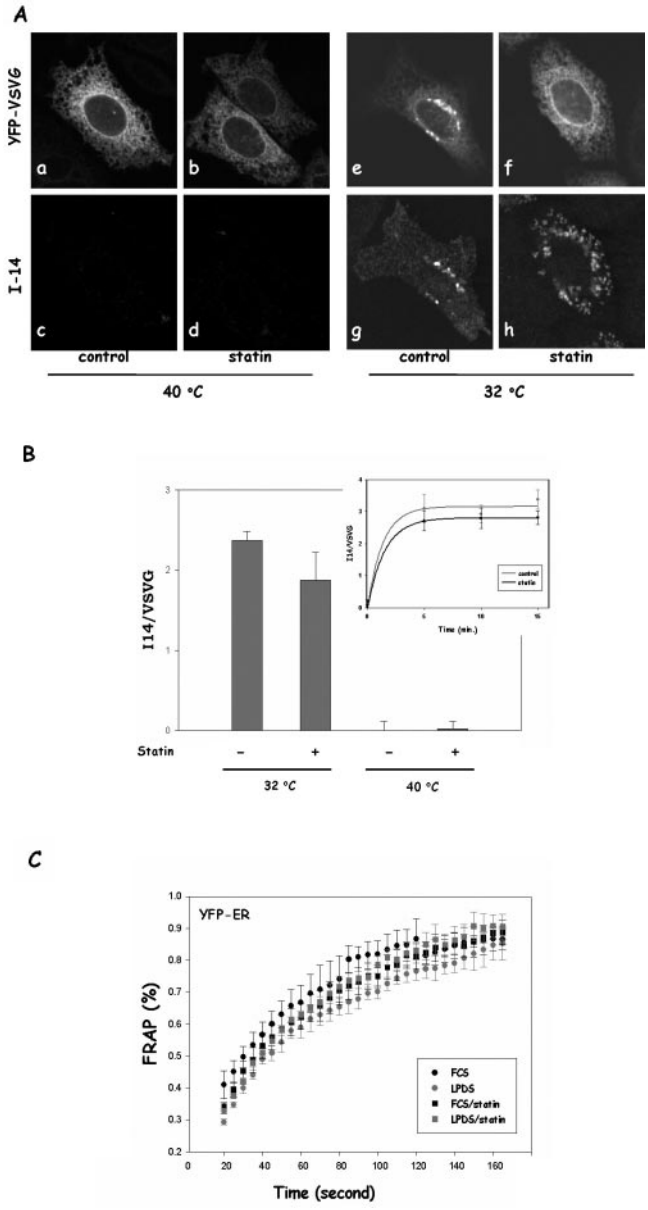

Figure 7. VSVG folding in statin-treated cells is largely normal. (A) CHO cells grown in LPDS were transfected with YFP-VSVG and incubated at 39.5°C overnight. Cells were then incubated at 39.5°C for an additional hour with or without 40 μM lovastatin. Some of the cells were fixed immediately (a–d), whereas other cells were transferred to 32°C incubator for 15 min (e–h) before fixation. Cells were then immunostained with I14, a mAb that only recognizes correctly folded VSVG. I14 was recognized by Alexa594 anti-mouse secondary antibody. (B) Fluorescent intensities of I14 immunostained cells were quantified. For each treatment, five images from random fields of cells were taken with a 10× objective for YFP (514 nm) and I14 (594 nm). After background subtraction, corresponding images were divided (594/514), and fluorescent intensities were calculated for each image. The bars represent the average of five random fields, and error bars are the SDs. I14 staining was also measured in cells that incubated at 32°C for 5, 10, and 15 min (inset). (C) CHO cells expressing YFP-ER were treated with or without 40 μM lovastatin for 1 h before FRAP experiments. The fluorescence intensities from photobleached spots were plotted as percentage of prebleach intensity in the same area against time. Each curve represents the average from five to 10 cells. Error bars are SEM.

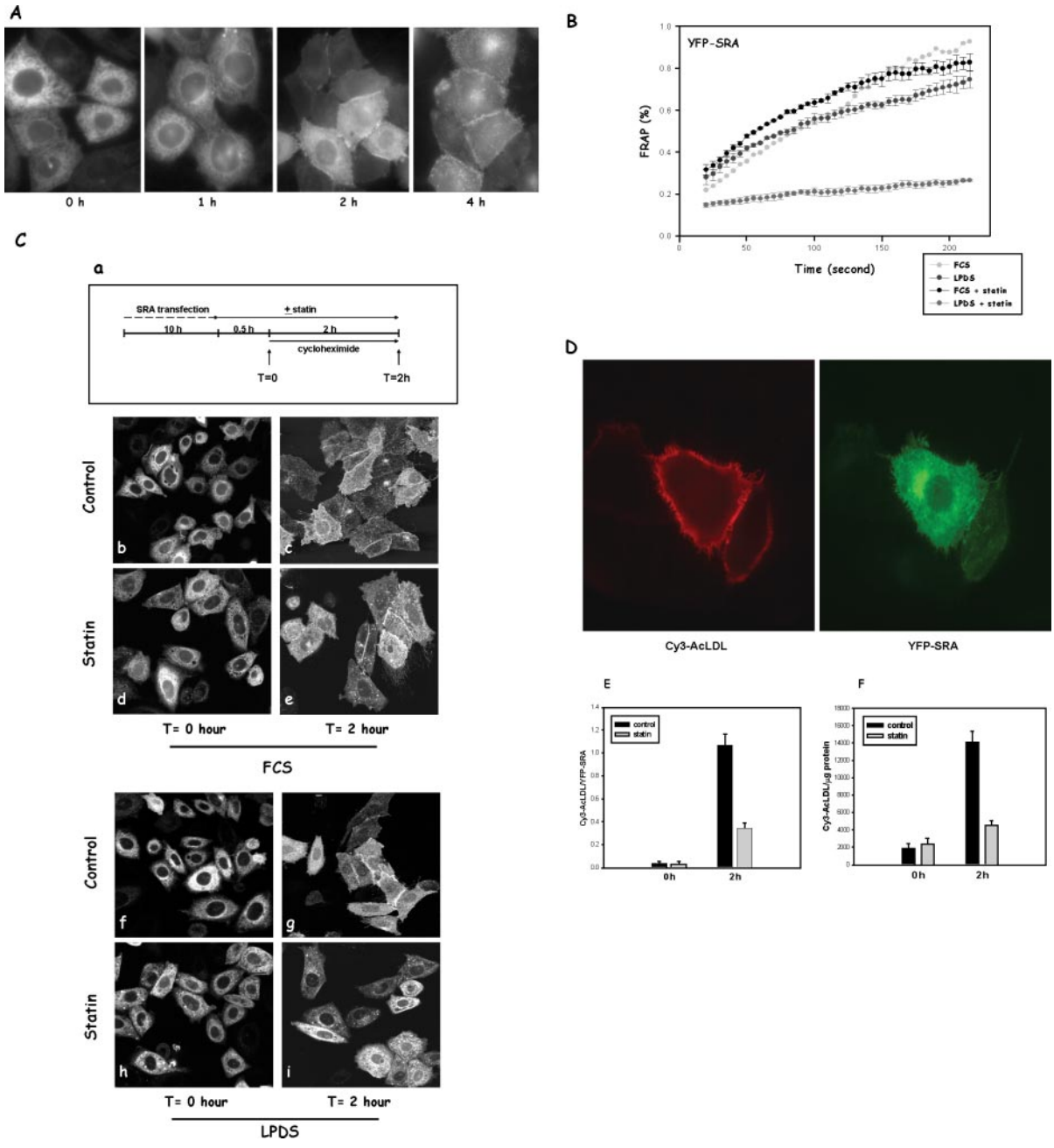

Figure 8. Cholesterol depletion by statin also impairs lateral mobility of SRA, and, concurrently, its transport from the ER. (A) YFP-SRA transport. CHO cells were transfected with YFP-SRA for 10 h, with or without statin in the last hour. Cycloheximide was added (0 h), and cells were incubated for additional 1, 2, and 4 h before microscopy observations. (B) Quantitative analysis of YFP-SRA fluorescence recovery. CHO cells expressing YFP-SRA were treated with or without 40 μM lovastatin for 1 h before FRAP experiments. The recovery of fluorescence intensities was analyzed similarly as in Figure 5B. (C) SRA transport from the ER. Following a protocol illustrated in a, CHO cells were transfected with SRA for 10 h in media containing either FCS or LPDS and then treated with statin for 30 min. Some cells were fixed right away (t = 0 h; b, d, f, and h), whereas the rest of the cells were incubated for additional 2 h in the presence of 20 μg/ml cycloheximide before confocal observation (t = 2 h; c, e, g, and i). (D) Cy3-acetyl-LDL surface binding in single cells. Cells were transfected with YFP-SRA for 10 h before cooling down on ice for 4°C binding. Cells were then imaged for both Cy3 and YFP. (E) The ratio of total fluorescent intensities of Cy3 and YFP was taken from each individual cell. Data are presented as an average of ratio from >50 cells and SEM. (F) Cy3-acetyl-LDL surface binding. Cells transfected with YFP-SRA were incubated with 10 μg/ml Cy3-acetyl-LDL for 30 min on ice, and, after rinsing with PBS, lysed with 1% TX-100/SDS. Cy3 in the lysates was analyzed with fluorospectrometry, and cellular protein was by Lowry assay. Data are presented as fluorescence intensity (arbitrary unit)/cellular protein (milligram), and averages of triplicates plus SD. All the experiments were repeated at least twice.

the majority of SRA was seen in the ER. When these cells were chased in the presence of cycloheximide, SRA was gradually transported out of the ER and onto the plasma membrane. After 2-h chase, a significant amount of SRA was located on the plasma membrane, and by 4 h the majority of SRA had reached the plasma membrane. This indicates that this particular YFP-SRA construct can successfully traffic to its final destination, the plasma membrane, the location

where untagged SRA was found (Zha *et al*., 1997; Terpstra *et al*., 2000). Little YFP-SRA remaining in the ER after 4-h chase also ensured that YFP-SRA was correctly folded. The above-mentioned observations nevertheless showed that YFP-SRA moves relatively slowly from the ER to the plasma membrane. This characteristic enabled us to select a time window (a few hours after transfection) in which YFP-SRA was only seen in the ER and to perform FRAP on these cells with or without statin treatment. We found that, almost identical to VSVG, SRA lost its lateral mobility when LPDS-grown cells were briefly treated with statin (Figure 8B). Once again, statin had little effect on cells grown in FCS. Interestingly, we noticed that even without statin SRA seems to recover much slower than VSVG (~60% recovery at 160 s versus nearly 100% for VSVG), indicating an intrinsically slower lateral mobility of SRA on the ER membrane.

We then quantitatively analyzed YFP-SRA transport from the ER. First, taking advantage of SRA's slow transport from the ER, we designed a morphological analysis protocol to study the transport of SRA from the ER. As shown in Figure 8C, a, we first pretreated cells grown in either FCS or LPDS with statin for 30 min and then added cycloheximide to block new protein synthesis for 2 h in the presence of statin. We reasoned that existing SRA should continuously exit ER during these 2 h, and the degree of ER depletion of SRA could be used as a measure of transport from the ER. As shown in Figure 8C, right before cycloheximide was added (t = 0; Figure 8C, b, d, f, and h), SRA could be seen mainly in the ER occasionally with a minor fraction in the Golgi. The outline of the nuclear envelope was highly visible: an indication of predominant ER localization of SRA at this point. A 30-min statin pretreatment did not significantly influence SRA distribution in either FCS- or LPDS-grown cells (Figure 8C, d and h). On 2-h chase in the presence of cycloheximide, a significant portion of SRA had exited the ER in control cells (FCS or LPDS-grown). Nuclei were no longer predominantly visible in these cells and most of SRA were either in punctate structures, presumably secretory vesicles, or on the plasma membrane (Figure 8C, c and g). These observations indicate that during the 2-h chase, a significant portion of SRA was transported from the ER and had reached the plasma membrane. When LPDS-grown cells were treated with statin (Figure 8C, i), however, the 2-h chase did not produce significant transport of SRA from the ER: nuclei including nuclear envelope were still predominantly visible, and there was virtually no plasma membrane staining. These observations strongly suggested an impaired SRA transport from the ER in these cells, similar to our earlier observation with VSVG. Interestingly, in FCS-grown cells treated with statin (Figure 8C, e), a significant amount of SRA had departed from ER and reached the plasma membrane by the end of the 2-h chase in most cells. Nuclei in some of the cells, however, are more visible than in control cells, suggesting a minor influence by statin.

Based on these observations, we double-blind scored a large number of cells (~1000 cells for each treatment). This was performed by taking fluorescent images from at least six random fields of cells for each treatment with a 10× objective. Cells were then classified as the ER type if they have a clearly defined nuclear outline or the plasma membrane (PM) type if the nucleus was no longer visible. The result is shown in Table 1. Right before cycloheximide was added (t = 0 h), ~80% of the cells had well outlined nuclei. After the 2-h chase in the presence of cycloheximide (t = 2 h), however, only ~20% of cells that still had visible nuclei in control cells, both FCS- and LPDS-grown cells, indicating that SRA was effectively transported out of the ER in the majority of the cells during this period. In contrast, when LPDS-grown cells were treated with statin during this 2-h chase, SRA was retained in the ER in ~70% of the cells, almost identical to the distribution before the chase (t = 0 h). SRA transport from the ER in FCS-grown cells was slightly affected by statin (34% with ER phenotype after 2-h chase), again similar to VSVG transport in these cells.

Table 1. SRA transport from the ER

Time (h)	Treatment	ER (cell no.)	Total (%)	PM (cell no.)	Total (%)
0	Control (FCS)	823	80	214	20
	Statin (FCS)	667	83	138	17
	Control (LPDS)	594	83	120	17
	Statin (LPDS)	883	83	178	17
2	Control (FCS)	165	20	692	80
	Statin (FCS)	339	34	643	66
	Control (LPDS)	143	19	592	81
	Statin (LPDS)	752	70	327	30

Data are representative results from three independent experiments.

To further verify our morphological analysis, we measured 4°C binding of Cy3-labeled acetyl-LDL (Cy3-AcLDL), a known ligand to untagged SRA (Zha *et al*., 1997). CHO cells do not express a significant level of SRA, and there was no significant Cy3-AcLDL binding in these cells. When we expressed YFP-SRA in these cells, however, Cy3-AcLDL was seen strongly bound to the surface of cells expressing YFP-SRA (Figure 8D). This ensured us that YFP-SRA had also retained the functionality of its untagged version. We first measured Cy3-AcLDL binding at the single cell level by taking fluorescent intensity ratios of Cy3 (acetyl-LDL bound) and YFP (SRA expressed) from individual cells and found that surface binding of Cy3-AcLDL was significantly diminished in statin-treated cells (Figure 8E). We also biochemically analyzed surface bound Cy3-AcLDL by lysing cells and measuring Cy3 signal in cell lysates by using fluorospectrometry. As shown in Figure 8F, the result is essentially identical to single cell analysis. Given the fact that YFP-SRA was seen mainly in the ER and not significantly retained in the Golgi in statin-treated cells (Figure 8C, i), inhibition of Cy3-AcLDL binding is most likely due to defective ER-to-Golgi transport. We therefore concluded that SRA, also a secretory membrane protein, was prevented from exiting the ER effectively in these cholesterol-depleted cells.

Together with our earlier observations with VSVG, our results demonstrate that cholesterol depletion by statin has a general effect on the lateral mobility of transmembrane proteins in the ER. A decreased lateral mobility can be correlated with impaired vesicular transport of these proteins from the ER. It is, therefore, most likely that the decreased lateral mobility prevents these membrane proteins from effectively reaching ER exit sites, leading to impaired ER-to-Golgi transport.

Cholesterol Depletion Renders VSVG Detergent Insoluble in the ER

So far, we provided evidence that inhibition of cholesterol synthesis in the ER causes impaired vesicular transport of membrane proteins. This is most likely because of the depletion of cholesterol from ER membrane, leading to decrease in lateral mobility of transmembrane proteins. The precise mechanism by which cholesterol depletion influ-

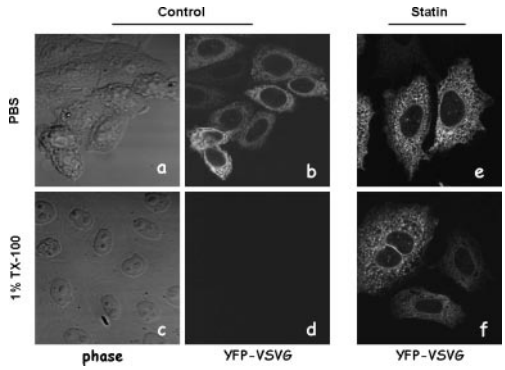

Figure 9. Cholesterol depletion by statin renders VSVG-detergent insoluble in the ER. CHO cells expressing YFP-VSVG were incubated at 39.5°C overnight. Cells were then either treated with 40 μM lovastatin for 1 h (e and f) or without lovastatin (a–d). Some of the cells were fixed and observed immediately (a, b, and e). The rest of the cells were cooled on ice and incubated with ice-cold 1% TX-100 for 30 min on ice (c, d, and f) before microscopic observation.

ences lateral mobility of these proteins is not immediately clear. Cholesterol depletion, however, is likely to impact on physical properties of the ER membrane. These altered physical properties can probably impact on protein conformation or interactions (Killian, 1998), which may in turn influence their lateral mobility on the ER membrane.

We therefore looked into whether cholesterol depletion influences detergent solubility of VSVG. VSVG is a nonraft protein known to be soluble in cold TX-100 even after being transported to the plasma membrane (Keller *et al*., 2001). When we treated LPDS-grown cells with 1% cold TX-100, ER YFP-VSVG in control cells was readily removed as expected (Figure 9d). In contrast, YFP-VSVG is more resistant to cold TX-100 treatment in statin-treated cells (Figure 9f). Cold TX-100 readily solubilized VSVG in FCS-grown cells when treated with statins (our unpublished data). It thus seemed that cholesterol depletion by statin affected the properties of VSVG in the ER. This alteration may have significant influence on VSVG ER lateral mobility.

DISCUSSION

In this report, we provide evidence that cholesterol depletion in the ER membrane profoundly impairs vesicular transport of membrane proteins from the ER. When cells are grown in lipoprotein-depleted (LPDS) media, de novo synthesis in the ER is the main source of cellular cholesterol. Newly synthesized cholesterol is rapidly transported out of ER to other cellular membranes (Ikonen *et al*., 2004), resulting in the low cholesterol content in ER membrane at steady state. Acute inhibition of the cholesterol synthesis in the ER of the LPDS-grown cells should thus lead to depletion of cholesterol initially from the ER membrane. This is supported by our observations that statin only caused rather minor depletion of total cellular cholesterol and had no visible effect on cholesterol in the plasma membrane, the endosomes, and the Golgi, judging from filipin staining. In addition, the ER is the only cellular location along the biosynthesis transport pathway most significantly altered by such acute statin treatment. Moreover, supplementing statin-treated cells with low amounts of cholesterol can completely rescue VSVG transport from the ER. That cholesterol alone could rescue the vesicular transport from the ER also argues against the possibility that other by-products of the mevalonate pathway may act as effectors of vesicular transport. We therefore concluded that acute inhibition of cholesterol synthesis in the ER specifically decreases ER cholesterol levels and thereby impairs vesicular transport of membrane proteins from the ER.

Direct measurement of the cholesterol content in the ER membrane is technically difficult. Any minor contamination from other cellular membranes could significantly alter the analysis. We observed that a very small amount of cholesterol in the media (1 μg/ml) could completely reverse the effect of statin in live cells, implying that the ER membrane is sensitive to minor alterations of the cholesterol contents in its environment. Cell fractionation, a commonly used method to separate the ER membrane, would inevitably perturb this environment and prevent accurate measurement of cholesterol in its native distribution.

We also provide evidence that cholesterol depletion by statin under our experimental conditions has a rather minor effect on the Golgi. By and large, the Golgi is structurally and functionally intact within our experimental time frame. This is supported by immunostaining of various Golgi markers and coat proteins. We demonstrate that VSVG could be transported from the Golgi to the plasma membrane relatively normally under our cholesterol depletion conditions, although we could not exclude some minor quantitative effects on the process. Interestingly, a previous report demonstrated that Golgi function was highly sensitive to its cholesterol contents, using a cell-free Golgi transport assay (Stuven *et al*., 2003). At the whole cell level, however, cholesterol depletion, particularly by MCD, has only rather moderate effects on vesicular transport from the Golgi to the plasma membrane. For example, after removing >60% of cellular cholesterol with MCD, VSVG transport was perfectly normal and hemagglutinin movement to the plasma membrane was partially inhibited (Keller and Simons, 1998). Only when a very high concentration of MCD was used did the Golgi become significantly affected (Hansen *et al*., 2000). These observations raise two not mutually exclusive possibilities. First, cholesterol in the Golgi is stably sequestered compared with in other cellular locations. Second, cholesterol depletion by MCD may have much more limited influence on intracellular organelles than on the plasma membrane. Statin treatment used in this study is most likely depleting cholesterol within the cells, and the depletion is relatively moderate. Given the relatively short duration of our experiments, it would not be surprising at all that Golgi cholesterol would only be minimally disturbed under our experimental conditions. This view seems to be supported by filipin staining (Figure 1A). Our observations, therefore, strongly dismiss the possibility of Golgi structural disintegration by statins and thus the possibility that impaired transport from ER is secondary to impaired Golgi function. The fact that VSVG could not efficiently reach ERGIC at 15°C in cells treated with statin should further strengthen our conclusion. It is also important to point out that, although cholesterol depletion significantly reduces ER-to-Golgi trafficking, the vesicular transport is still occurring. This low level of ER-to-Golgi transport could be critical in maintaining the Golgi structure. It could also be critical in sending SREBP to the Golgi for processing even when ER cholesterol is severely depleted.

Our conclusion that vesicular transport of VSVG is sensitive to ER cholesterol apparently differs from a previous study where cholesterol depletion by 30-min incubation with MCD did not affect ER-to-Golgi transport (Keller and Simons, 1998). We were able to confirm in CHO cells that identical MCD treatment indeed had no influence on VSVG ER-to-Golgi trans-

port (our unpublished observations). However, we attribute this to, although extremely powerful in depleting cellular cholesterol, MCD mainly affecting the plasma membrane (Yancey *et al*., 1996). It may take time for this depletion to be sensed by the ER. It remains possible that ER cholesterol was not significantly altered during this 30-min MCD incubation, which would leave ER-to-Golgi transport unaffected. Interestingly, results presented in the same work have shown that 60% cholesterol depletion by MCD did not influence VSVG transport from the Golgi to the plasma membrane at all (Keller and Simons, 1998). This further suggests that MCD could not deplete cholesterol from intracellular organelles with the equal efficiency as from the plasma membrane.

We presented evidence here that cholesterol depletion results in a significant decrease of lateral mobility of membrane proteins. The diffusion coefficient, *D*, for VSVG lateral mobility in the ER, 0.085 ± 0.012 $\mu m^2/s$, is within the range of other ER membrane proteins that have been studied (0.1–0.5 $\mu m^2/s$) (Haggie *et al*., 2002). The *D* for VSVG in COS cells was reported to be 0.4 $\mu m^2/s$ (Nehls *et al*., 2000). Our measurement is therefore in the same order as in COS cells. The slight difference is likely because of cell type differences or different VSVG constructs. We indeed obtained a faster *D* with our YFP-VSVG construct in COS cells (0.17 ± 0.025 $\mu m^2/s$) (unpublished observations), suggesting variations in the ER membrane environment in different cell types. Importantly, *D* for VSVG in LPDS-grown, statin-treated CHO cells was significantly smaller (0.014 ± 0.002 $\mu m^2/s$), indicating a severe impairment of VSVG lateral diffusion in these cells.

It is not immediately clear how cholesterol depletion in the ER impairs lateral mobility of membrane proteins. The majority of the cellular cholesterol is on the plasma membrane where it provides the physical properties necessary for maintaining structural integrity of the plasma membrane. In recent years, cholesterol was also thought to play a central role in organizing microdomains on the plasma membrane, such as "rafts" (Simons and Ikonen, 2000). These microdomains seem to be tied to a large number of cellular processes. Cholesterol depletion from the plasma membrane by MCD, for example, has shown to abolish many important cellular processes, including signal transduction (Simons and Ikonen, 2000). Interestingly, cholesterol depletion from the plasma membrane severely reduced the lateral mobility of class 1 MHC molecules, type 1 transmembrane proteins (Kwik *et al*., 2003). This effect was attributed to increased formation of actin cytoskeleton meshwork, likely a compensatory mechanism to reinforce the plasma membrane weakened by cholesterol depletion.

The ER membrane is cholesterol poor. Cholesterol content in the ER membrane, however, seems to be stringently controlled. It is on the ER membrane where most of the cholesterol regulatory proteins, such as SREBP and acyl-coenzyme A:cholesterol acyltransferase, reside. These proteins function to regulate cholesterol synthesis/uptake and sequestration of excess free cholesterol. It is probably necessary for mammalian cells to use these molecular machineries to tightly control cellular cholesterol levels, including in the ER membrane. A high sensitivity of the ER membrane to its cholesterol content might thus be advantageous if this membrane were to function as a cellular cholesterol sensor. Studies on model membranes with lipid compositions similar to those in the ER have indeed shown that a number of physical properties are highly sensitive to small cholesterol alterations (Lemmich *et al*., 1997). In these cholesterol poor-model membranes, a slight variation in cholesterol relative to the total lipid content, for example, from 4 to 2%, could cause a profound reduction in membrane thickness.

The impaired transport of membrane proteins from the ER shown in this study is likely because of decreased lateral mobility of these proteins on the ER membrane. This relative immobility in principle would prevent these proteins from efficiently reaching the ER exit sites even if they have adequate cargo targeting machineries, providing that lateral diffusion is the rate-limiting step for these proteins. Statin treatment in this study decreased the diffusion coefficient of VSVG by ~80% in comparison with control (Figure 6C). Interestingly, ER-to-Golgi transport of VSVG in these statin-treated cells is also inhibited by a similar degree (Figure 2B). Although a slightly less efficient folding of VSVG in statin-treated cells could contribute to unsuccessful ER exit; however, quantitatively it would account only for ~4% of failed VSVG transport, because 20% of VSVG that managed to reach the ER exit sites (presumably 20% of the control) is likely misfolded. It is therefore tempting to suggest that the relatively high mobility of membrane proteins in the ER membrane is necessary although not sufficient for secretory membrane proteins to effectively reach the cargo exit site and thus be efficiently transported from the ER.

Although we demonstrated that ER exit sites are structurally intact, we cannot rule out the possibility that cholesterol depletion functionally impairs ER exit machinery. For example, a change in membrane thickness could affect sorting mechanisms at ER exit sites, which could become rate limiting for VSVG and for other membrane proteins. Currently, we do not know whether cholesterol in the ER is homogeneously distributed or with higher concentrations in some particular locations, such as in the ER exit sites. Cholesterol depletion could then have differential effects among these locations, similar to its effect on caveolae and clathrin-coated pits on the plasma membrane.

It is also currently not clear how membrane proteins lose their lateral mobility. The decrease in lateral mobility is not likely to be because of faulty interactions with chaperone complexes known to cause aggregation of membrane proteins (de Silva *et al*., 1993), because most SRA in our transport experiments was formed before statin treatment. In addition, misfolded VSVG has also been shown to diffuse similarly to correctly folded VSVG (Nehls *et al*., 2000). The only glimpse of information we have at the moment is that ER VSVG in statin-treated cells is more resistant to TX-100. This insolubility could suggest that VSVG is more aggregated under cholesterol depletion condition, perhaps because of altered protein–membrane interactions. If we assume that ER membrane behaves somewhat similar to model membranes, cholesterol depletion by statin could result in membrane thinning (Lemmich *et al*., 1997). One of the immediate effects of such membrane thinning would be the hydrophobic mismatch between transmembrane domains (TMDs) of membrane proteins and their surrounding membranes (Killian, 1998). Membrane thinning thus in principle could generate an energetically unfavorable exposure of TMDs to the aqueous environment. This would lead to aggregation of membrane proteins. Alternatively, cholesterol depletion could increase ER membrane rigidity, similar to low cholesterol model membranes, which could in turn prevent membrane proteins from diffusing freely on the membrane. We however failed to find such evidence by measuring 1,6-diphenyl-1,3,5-hexatriene rotational mobility in the ER membrane (our unpublished data). Further studies are necessary to understand the factors governing membrane protein lateral mobility on the ER membrane under cholesterol-depleted conditions.

In summary, we provide evidence here for the first time that cholesterol depletion in the ER leads to impaired ER-to-Golgi vesicular transport of membrane proteins. This is

likely because of diminished lateral mobility of these membrane proteins. Cholesterol is thus necessary to keep membrane proteins mobile in the ER, likely by maintaining adequate physical properties of the ER membrane.

ACKNOWLEDGMENTS

We thank Dr. Murray Huff for discussions and suggestions at the early stage of the project. We are also indebted to Dr. Robert Hache for sharing microscopy system, to Dr. Catherine Morris for critically reading the manuscript, and to Stephanie Bell for assistance in immunofluorescent microscopy. This work is supported by grants from Heart and Stroke Foundation of Canada, Heart and Stroke Foundation of Ontario (NA 5246), Canada Institutes of Health Research, Canada Innovation Foundation, and by a start-up fund from Ottawa Health Research Institute.

REFERENCES

Adams, C. M., Goldstein, J. L., and Brown, M. S. (2003). Cholesterol-induced conformational change in SCAP enhanced by Insig proteins and mimicked by cationic amphiphiles. Proc. Natl. Acad. Sci. USA *100*, 10647–10652.

Antonny, B., and Schekman, R. (2001). ER export: public transportation by the COPII coach. Curr. Opin. Cell Biol. *13*, 438–443.

Bergmann, J. E. (1989). Using temperature-sensitive mutants of VSV to study membrane protein biogenesis. Methods Cell Biol. *32*, 85–110.

Bradfute, D. L., and Simoni, R. D. (1994). Non-sterol compounds that regulate cholesterogenesis. Analogues of farnesyl pyrophosphate reduce 3-hydroxy-3-methylglutaryl-coenzyme A reductase levels. J. Biol. Chem. *269*, 6645–6650.

Brown, M. S., and Goldstein, J. L. (1997). The SREBP pathway: regulation of cholesterol metabolism by proteolysis of a membrane-bound transcription factor. Cell *89*, 331–340.

Brown, M. S., and Goldstein, J. L. (1999). A proteolytic pathway that controls the cholesterol content of membranes, cells, and blood. Proc. Natl. Acad. Sci. USA *96*, 11041–11048.

Corvera, E., Mouritsen, O. G., Singer, M. A., and Zuckermann, M. J. (1992). The permeability and the effect of acyl-chain length for phospholipid bilayers containing cholesterol: theory and experiment. Biochim. Biophys. Acta *1107*, 261–270.

de Silva, A. M., Balch, W. E., and Helenius, A. (1990). Quality control in the endoplasmic reticulum: folding and misfolding of vesicular stomatitis virus G protein in cells and in vitro. J. Cell Biol. *111*, 857–866.

de Silva, A., Braakman, I., and Helenius, A. (1993). Posttranslational folding of vesicular stomatitis virus G protein in the ER: involvement of noncovalent and covalent complexes. J. Cell Biol. *120*, 647–655.

Goldstein, J. L., and Brown, M. S. (1990). Regulation of the mevalonate pathway. Nature *343*, 425–430.

Haggie, P. M., Stanton, B. A., and Verkman, A. S. (2002). Diffusional mobility of the cystic fibrosis transmembrane conductance regulator mutant, delta F508-CFTR, in the endoplasmic reticulum measured by photobleaching of GFP-CFTR chimeras. J. Biol. Chem. *277*, 16419–16425.

Hall, A. (1998). Rho GTPases and the actin cytoskeleton. Science *279*, 509–514.

Hancock, J. F., Magee, A. I., Childs, J. E., and Marshall, C. J. (1989). All ras proteins are polyisoprenylated but only some are palmitoylated. Cell *57*, 1167–1177.

Hansen, G. H., Niels-Christiansen, L. L., Thorsen, E., Immerdal, L., and Danielsen, E. M. (2000). Cholesterol depletion of enterocytes. Effect on the Golgi complex and apical membrane trafficking. J. Biol. Chem. *275*, 5136–5142.

Heino, S., Lusa, S., Somerharju, P., Ehnholm, C., Olkkonen, V. M., and Ikonen, E. (2000). Dissecting the role of the Golgi complex and lipid rafts in biosynthetic transport of cholesterol to the cell surface. Proc. Natl. Acad. Sci. USA *97*, 8375–8380.

Ikonen, E. (2001). Roles of lipid rafts in membrane transport. Curr. Opin. Cell Biol. *13*, 470–477.

Ikonen, E., Heino, S., and Lusa, S. (2004). Caveolins and membrane cholesterol. Biochem. Soc. Trans. *32*, 121–123.

Istvan, E. (2003). Statin inhibition of HMG-CoA reductase: a 3-dimensional view. Atheroscler. Suppl. *4*, 3–8.

Kappeler, F., Klopfenstein, D. R., Foguet, M., Paccaud, J. P., and Hauri, H. P. (1997). The recycling of ERGIC-53 in the early secretory pathway. ERGIC-53 carries a cytosolic endoplasmic reticulum-exit determinant interacting with COPII. J. Biol. Chem. *272*, 31801–31808.

Keller, P., and Simons, K. (1998). Cholesterol is required for surface transport of influenza virus hemagglutinin. J. Cell Biol. *140*, 1357–1367.

Keller, P., Toomre, D., Diaz, E., White, J., and Simons, K. (2001). Multicolour imaging of post-Golgi sorting and trafficking in live cells. Nat. Cell Biol. *3*, 140–149.

Killian, J. A. (1998). Hydrophobic mismatch between proteins and lipids in membranes. Biochim. Biophys. Acta *1376*, 401–415.

Kwik, J., Boyle, S., Fooksman, D., Margolis, L., Sheetz, M. P., and Edidin, M. (2003). Membrane cholesterol, lateral mobility, and the phosphatidylinositol 4,5-bisphosphate-dependent organization of cell actin. Proc. Natl. Acad. Sci. USA *100*, 13964–13969.

Lange, Y. (1991). Disposition of intracellular cholesterol in human fibroblasts. J. Lipid Res. *32*, 329–339.

Lefrancios, L., and Lyles, D. S. (1982). The interaction of antibody with the major surface glycoprotein of vesicular stomatitis virus. I. Analysis of neutralizing epitopes with monoclonal antibodies. Virology *121*, 157–167.

Lemmich, J., Mortensen, K., Ipsen, J. H., Hønger, T., Bauer, R., and Mouritsen, O. G. (1997). Effect of cholesterol in small amounts on lipid-bilayer softness in the region of the main phase transition. Eur. Biophys. J. *25*, 293–304.

Lusa, S., Heino, S., and Ikonen, E. (2003). Differential mobilization of newly synthesized cholesterol and biosynthetic sterol precursors from cells. J. Biol. Chem. *278*, 19844–19851.

Mukherjee, S., Zha, X., Tabas, I., and Maxfield, F. R. (1998). Cholesterol distribution in living cells: fluorescence imaging using dehydroergosterol as a fluorescent cholesterol analog. Biophys. J. *75*, 1915–1925.

Nehls, S., Snapp, E. L., Cole, N. B., Zaal, K. J., Kenworthy, A. K., Roberts, T. H., Ellenberg, J., Presley, J. F., Siggia, E., and Lippincott-Schwartz, J. (2000). Dynamics and retention of misfolded proteins in native ER membranes. Nat. Cell Biol. *2*, 288–295.

Pitas, R. E., Innerarity, T. L., Weinstein, J. N., and Mahley, R. W. (1981). Acetoacetylated lipoproteins used to distinguish fibroblasts from macrophages in vitro by fluorescence microscopy. Arteriosclerosis *1*, 177–185.

Presley, J. F., Ward, T. H., Pfeifer, A. C., Siggia, E. D., Phair, R. D., and Lippincott-Schwartz, J. (2002). Dissection of COPI and Arf1 dynamics in vivo and role in Golgi membrane transport. Nature *417*, 187–193.

Radhakrishnan, A., Sun, L. P., Kwon, H. J., Brown, M. S., and Goldstein, J. L. (2004). Direct binding of cholesterol to the purified membrane region of SCAP; mechanism for a sterol-sensing domain. Mol. Cell *15*, 259–268.

Schafer, W. R., and Rine, J. (1992). Protein prenylation: genes, enzymes, targets, and functions. Annu. Rev. Genet. *26*, 209–237.

Schweizer, A., Fransen, J. A., Bachi, T., Ginsel, L., and Hauri, H. P. (1988). Identification, by a mAb, of a 53-kD protein associated with a tubulo-vesicular compartment at the cis-side of the Golgi apparatus. J. Cell Biol. *107*, 1643–1653.

Sciaky, N., Presley, J., Smith, C., Zaal, K. J., Cole, N., Moreira, J. E., Terasaki, M., Siggia, E., and Lippincott-Schwartz, J. (1997). Golgi tubule traffic and the effects of brefeldin A visualized in living cells. J. Cell Biol. *139*, 1137–1155.

Siggia, E. D., Lippincott-Schwartz, J., and Bekiranov, S. (2000). Diffusion in inhomogeneous media: theory and simulations applied to whole cell photobleach recovery. Biophys. J. *79*, 1761–1770.

Silvius, J. R. (2003). Role of cholesterol in lipid raft formation: lessons from lipid model systems. Biochim. Biophys. Acta *1610*, 174–183.

Simons, K., and Ikonen, E. (2000). How cells handle cholesterol. Science *290*, 1721–1726.

Simons, K., and Toomre, D. (2000). Lipid rafts and signal transduction. Nat. Rev. Mol. Cell Biol. *1*, 31–39.

Stuven, E., Porat, A., Shimron, F., Fass, E., Kaloyanova, D., Brugger, B., Wieland, F. T., Elazar, Z., and Helms, J. B. (2003). Intra-Golgi protein transport depends on a cholesterol balance in the lipid membrane. J. Biol. Chem. *278*, 53112–53122.

Terpstra, V., van Amersfoort, E. S., van Velzen, A. G., Kuiper, J., and van Berkel, T. J. (2000). Hepatic and extrahepatic scavenger receptors: function in relation to disease. Arterioscler. Thromb. Vasc. Biol. *20*, 1860–1872.

Van Aelst, L., and D'Souza-Schorey, C. (1997). Rho GTPases and signaling networks. Genes Dev. *11*, 2295–2322.

Yancey, P. G., Rodrigueza, W. V., Kilsdonk, E. P., Stoudt, G. W., Johnson, W. J., Phillips, M. C., and Rothblat, G. H. (1996). Cellular cholesterol efflux mediated by cyclodextrins. Demonstration of kinetic pools and mechanism of efflux. J. Biol. Chem. *271*, 16026–16034.

Zha, X., Tabas, I., Leopold, P. L., Jones, N. L., and Maxfield, F. R. (1997). Evidence for prolonged cell-surface contact of acetyl-LDL before entry into macrophages. Arterioscler. Thromb. Vasc. Biol. *17*, 1421–1431.